

Myosin light chain phosphorylation is required for peak power output of mouse fast skeletal muscle in vitro

Joshua Bowslaugh¹ · William Gittings¹ · Rene Vandenboom¹

Received: 19 July 2016 / Revised: 13 October 2016 / Accepted: 18 October 2016 / Published online: 28 November 2016
© Springer-Verlag Berlin Heidelberg 2016

Abstract The skeletal myosin light chain kinase (skMLCK) catalyzed phosphorylation of the myosin regulatory light chain (RLC) is associated with potentiation of force, work, and power in rodent fast twitch muscle. The purpose of this study was to compare concentric responses of EDL from wild-type (WT) and skMLCK devoid (skMLCK^{-/-}) muscles at a range of shortening speeds (0.05 to 0.70 V_{max}) around that expected to produce maximal power (in vitro, 25 °C) both before (unpotentiated) and after (potentiated) a potentiating stimulus (PS). When collapsed across all speeds tested, neither unpotentiated force, work, or power differed between genotypes (all data $n = 10$, $P < 0.05$). In contrast, although both genotypes displayed speed-dependent increases, these increases were greater for WT than skMLCK^{-/-} muscles. For example, when collapsed across the six fastest speeds we tested, both concentric force and power were increased 30–34 % in WT but only 15–17 % in skMLCK^{-/-} muscles. In contrast, at the two slowest speeds, these parameters were increased in WT but decreased in skMLCK^{-/-} muscles (8–10 and 7–9 %, respectively). Intriguingly, potentiation of concentric force and power was optimal near speeds producing maximal power in both genotypes. Because the PS elevated RLC phosphorylation above resting levels in WT but not in skMLCK^{-/-} muscles, our data suggest that skMLCK-catalyzed phosphorylation of the RLC is required for maximal concentric power output of mouse EDL muscle stimulated at high frequency in vitro.

Keywords Regulatory light chains · Length ramps · Mean power · Extensor digitorum longus · Concentric force · Work

Introduction

Terrestrial locomotion is essential for survival. As such skeletal muscle must generate and sustain force, work, and power across an almost infinite performance envelope in terms of muscle load, shortening trajectory, shortening speed, and activation level [23]. Given this requirement, it is perhaps not surprising that the mammalian fast muscle phenotype has evolved the ability to potentiate. Manifest as a contraction history-dependent increase in concentric force, work, or power, potentiation has been demonstrated in myriad rat [1, 2, 25, 26, 28] and mouse [13, 15, 18, 19, 41] skeletal muscle models. Because this state develops rapidly and dissipates slowly with the onset and cessation of contractile activity, respectively, potentiation may be the normal working state of fast skeletal muscle [9] (see also [36]).

From a teleological perspective, multiple or redundant mechanisms for potentiation should exist if this outcome is important for enhancing muscle function in vivo. Indeed, recent work using knockout and transgenic mouse muscle models suggest that such biological degeneracy does exist (e.g., [33, 42]). For example, myriad lines of evidence suggest that the primary mechanism for potentiation is phosphorylation of the myosin regulatory light chain (RLC) as catalyzed by myosin light chain kinase (skMLCK) [35]. For example, studies performed on permeabilized skeletal muscle fibers show that the addition of skMLCK and subsequent phosphorylation of the RLC increase the Ca^{2+} sensitivity of steady state force development (e.g., [31]). From a mechanistic viewpoint, phosphorylation of the RLC may alter myosin structure/position on the thick filament, a change proposed to increase

✉ Rene Vandenboom
rvandenboom@brocku.ca

¹ Center for Bone and Muscle Health, Faculty of Applied Health Sciences, Brock University, 1812 Sir Isaac Brock Way, St. Catharines, ON L2S 3A1, Canada

motor domain binding to actin (e.g., [4]). Importantly, although these studies account for the strong temporal associations obtained between stimulation-induced elevations in RLC phosphorylation and isometric twitch force potentiation in a number of rodent muscle models (see [40], and references therein), they do not necessarily exclude other mechanisms for potentiation. For example, as first shown by Zhi et al. [42] and subsequently confirmed by Gittings et al. [14], skMLCK devoid muscles unable to phosphorylate the RLC retain a residual level of isometric twitch force potentiation under some conditions. Thus, although potentiation is often proportional to stimulation-induced levels of RLC phosphorylation, both skMLCK-dependent and skMLCK-independent forms of potentiation may operate in wild-type muscles. Moreover, up-regulation of skMLCK enzyme content in mouse slow twitch muscle such as the soleus does not produce potentiation [33]. As a result, potentiation may require specific protein expression encapsulated by the murine fast twitch muscle gene program.

The relative contribution of RLC phosphorylation-dependent and phosphorylation-independent mechanisms to the potentiation displayed by wild-type muscles is still largely unknown. In the absence of RLC phosphorylation, the potentiation deficit between wild-type and skMLCK devoid muscles may depend critically upon muscle-shortening speed. Thus, the purpose of this study was to compare the mechanical power of fully activated wild-type and skMLCK devoid muscles at a range of shortening speeds expected to produce peak power. We hypothesized that, in the absence of skMLCK catalyzed phosphorylation of the RLC, peak power would be reduced and the shortening speed at which peak power was attained would be altered compared to wild-type muscles.

Methods

All procedures utilized in this study received ethical approval from the Brock University Animal Care Committee. Adult male C57BL/6 wild-type (WT) mice (age 3–6 months; mass 27.6 ± 0.2 g) were ordered from Charles River Labs (St. Constant, QC), and skMLCK^{-/-} mice (age 2–5 months; mass 23.2 ± 1.2 g) were obtained from our own breeding colony at Brock University. Details regarding the generation and characterization of skMLCK devoid (skMLCK^{-/-}) have been previously presented [14, 42]. Mice were anesthetized with an intraperitoneal injection of sodium pentobarbital (60-mg/kg body mass) diluted with 0.9 % saline in a 1-mL syringe. The EDL muscle was then surgically excised and mounted in a jacketed vertical organ bath. The organ bath contained Tyrode's physiological solution [23] maintained at 25 °C, which was continuously oxygenated using a gas mix of 95 % O₂ and 5 % CO₂. Modeling work by Barclay [7] has verified that mouse EDL muscles maintained in this way

remain viable even when stimulated at high frequencies. Muscle stimulation was applied using flanking platinum electrodes, provided by a model 701B bi-phasic stimulator (Aurora Scientific Inc., Aurora, ON) with voltage set to 1.25 times the threshold required to active all fibers and elicit maximal twitch force. This was followed by a 30-min equilibration period, after which the optimal length for maximal isometric twitch force was determined (L_o). During experiments, muscle length and force data were monitored via LINUX software and controlled by a dual-mode servomotor (Model 305B, Aurora Scientific Inc., Aurora, ON). All experiments were collected at 2000 Hz and saved to computer for further analysis (ASI 600a software).

Experimental protocol The experimental protocol is illustrated in Fig. 1. Length ramps were applied to each muscle before and after a potentiating stimulus (PS) consisting of four volleys of 100-Hz stimulation of 400-ms duration within a 10-s time window; during this protocol, muscle length was held at L_o . This procedure was repeated four times per muscle, with consecutive protocols being separated by ~20 min to allow potentiation to dissipate between protocols. Two different ramp speeds were tested before and after each PS, a protocol allowing us to test eight different shortening speeds per muscle (of each genotype). Our use of multiple PS procedures to test different speeds within each muscle was validated by highly repeatable measures of both unpotentiated and potentiated force, work, and power at various points during each experiment (data not shown). For each PS, pre- and post-length ramps were matched for speed, although the sequence of length ramp speeds was randomized from muscle to muscle within each genotype.

Shortening ramps The different rates of ramp (i.e., shortening speed) used in these experiments ranged from 0.05 to 0.70 V_{max} , with all speeds scaled to an absolute shortening speed of 9.8 fiber lengths per second [14, 15]. For reporting purposes, shortening speeds over the slowest speed used were binned to the nearest 0.10 V_{max} . Each shortening ramp decreased muscle length from 1.05 to 0.90 L_o with the onset of muscle stimulation delayed so that concentric force always began at ~1.045 L_o . For each speed tested, a pair of shortening ramps, one "passive" and one "active," were applied at set times before and after the PS. This was done to account for changes in passive force caused by the PS. It has been shown previously that a sequence in which a passive-active ramp pair precedes a passive-active ramp without an intervening PS does not influence concentric responses of mouse EDL muscle in vitro at 25 °C [18]. During each active ramp, muscles were stimulated using a pair of pulses with a 10-ms interpulse interval (i.e., 100 Hz) for all speed conditions. Because we used different rates of ramp, the duration of shortening varied from 110 to 543 ms for the fastest to the slowest shortening speeds,

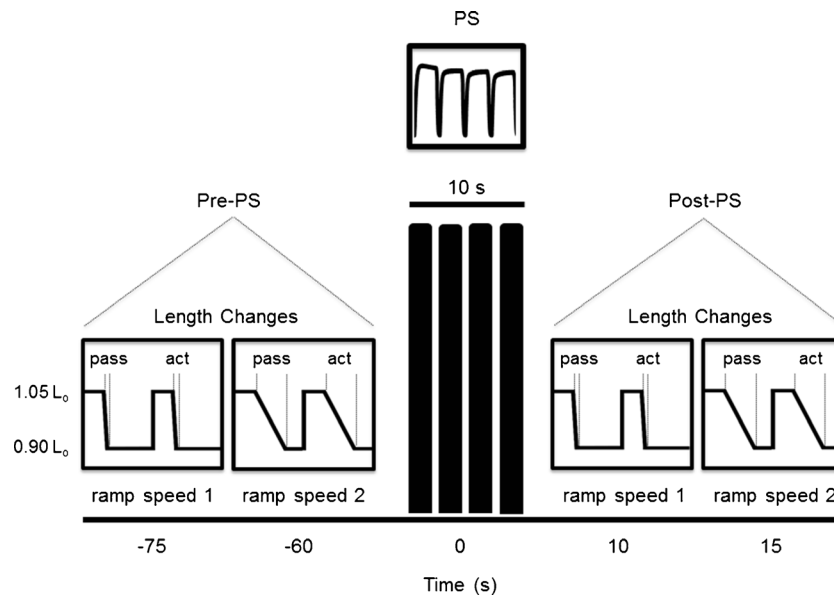


Fig. 1 Experimental design for collecting concentric force at different shortening speeds before and after a potentiating stimulus (PS) for wild-type (WT) and skeletal myosin light chain kinase devoid (skMLCK^{-/-}) muscles. Four identical potentiating stimuli (PS) were applied to each muscle at ~20-min intervals. Each PS consisted of four volleys of 100-Hz stimulation of 400-ms duration within an ~10-s window; muscle length was held at optimal length (i.e., 1.00 L_0) (see inset). Two different shortening speeds were assessed with each PS allowing us to assess the influence of potentiation on concentric force at eight different shortening speeds (0.05, 0.10, 0.20, 0.30, 0.40, 0.50, 0.60, and 0.70 V_{max}) per muscle of each genotype. As shown in the figure, two pairs of identical ramps, at each of two different speeds, were applied before and after each PS (0.50 and 0.30 V_{max} in example shown). The timing of these pairs was designed to minimize interference before but to capture the peak of potentiation after the PS, respectively. Although the rate of ramp (i.e., speed) was varied, shortening amplitude was fixed at 15 % L_0 (1.05–0.90 L_0). During the first of each of these ramps, the muscle was not stimulated and passive forces were recorded. During the second of these ramps, the

muscle was stimulated and total (passive + active) force was recorded. The active concentric force corresponding to each ramp speed (unpotentiated and potentiated) was obtained by subtracting passive force from total force; the magnitude of potentiation for each ramp speed was determined by dividing post-PS active force by pre-PS active force. Although passive ramps always preceded active ramps, the order of shortening speed was randomized between muscles both in terms of sequence around the PS as well as PS number (1–4). Muscles were frozen either 20 s or 20 min after the final PS procedure in each experiment to obtain stimulated (i.e., potentiated) and resting (i.e., unpotentiated) values for RLC phosphorylation, respectively. Other work from our lab has shown that repeatable levels of RLC phosphorylation may be obtained in response to multiple PS procedures [13]. Peak tetanic force declined 5–10 % from tetanus 1 to tetanus 4 within each PS for both genotypes. Vertical dotted lines depict the ramp duration (passive or active) for two different ramp speeds. Length records are simulations and not meant to represent actual speeds. Abbreviations: *pass*, passive ramps; *act*, active ramps

respectively. Muscles were always able to completely relax before the end of each shortening ramp. Muscles were not stimulated during passive ramps.

Analysis of force, work, power, and kinetics Concentric force, work, power, and the kinetics of force development and relaxation were assessed using identical methods in wild-type and skMLCK^{-/-} muscles. Total, passive, and active forces (concentric) were recorded during each isovelocity shortening ramp (active and passive). Active forces were obtained by subtracting the passive force response from the matching total force response with mean concentric force calculated as the arithmetic average from the initiation to the cessation of the active tension record. Muscle cross-sectional area (CSA) was determined by dividing muscle mass (g) by the product of its length (cm) while at L_0 and muscle density (1.06 g/cm³) [30] and expressed in mm² (see [20] for details). Stress (g/mm²) was determined by dividing tension (g) by muscle CSA. Muscle work was determined by calculating

the force-time integral (in joules) and normalizing this value to muscle mass (J/kg); mean power was calculated as force multiplied by shortening velocity, expressed in watts, and normalized to muscle mass (W/kg). The maximal rate of concentric force development ($+dF/dt$) and relaxation ($-dF/dt$) were determined by obtaining the first derivative of the active force record and expressed as mN/s.

Myosin RLC phosphorylation At the conclusion of each experiment, muscles were frozen in liquid nitrogen either 20 s or 20 min after the final PS and stored at -80 °C. These groups represented stimulated and resting levels of RLC phosphorylation, respectively ($n = 4$ for each group and genotype). We have previously shown that repeatable levels of RLC phosphorylation are produced in response to multiple PS procedures [13, 38]. Our current data shows that 20 min is a long enough time period to allow dephosphorylation of the RLC from stimulated to resting levels.

Western blotting Frozen muscles were subsequently thawed, then denatured using dithiothreitol (DTT) and trichloroacetic acid (TCA) and homogenized by mortar and pestle until a consistent mixture was obtained. After centrifugation at 2000 rpm for 2 min, the supernatant was poured off and the remaining pellet was then washed using ethyl ether to remove excess TCA. The pellet was then resuspended in a urea-based sample buffer and urea crystals were added, as necessary, to achieve complete saturation and solubilize the RLC of each sample. Following this, samples were pipetted into separate wells of a Bio-Rad minigel electrophoresis apparatus (10 μ L per sample) containing a polyacrylamide gel with the addition of glycerol for density. Gels were run for 85 min at 400 V and then transferred to a nitrocellulose membrane using a non-conducting gel-membrane cassette submerged in transfer buffer. After transfer, the membranes were washed with Tris-buffered saline + Tween 20 (TBST), followed by incubation in blocking buffer for 1 h to prevent blocking of non-specific protein binding. Lastly, the nitrocellulose gels were incubated with 1 $^{\circ}$ (1:7500) antibody (RLC) and were then stored overnight at \sim 4 $^{\circ}$ C. The next day, the membranes were washed with TBST to remove 1 $^{\circ}$ antibody, immediately followed by incubation with 2 $^{\circ}$ (1:10,000) goat anti-rabbit IgG-horseradish peroxidase (Santa Cruz Biotechnology, Inc.) in TBST for 1 h at room temperature. The membranes were then incubated with a detection buffer for 3 min and rinsed with dH $_2$ O before being placed in a FluorChem 5500 for exposure and photo-analysis.

Statistical analysis The data was checked for normality using a Shapiro-Wilk test. A two-way repeated measures ANOVA was used to test for the influence of shortening speed and activation state (unpotentiated vs potentiated) on each contractile measure for each genotype. A separate two-way factorial ANOVA (2 \times 8) was used to test for the influence of genotype and shortening speed on the relative change in each of the contractile measures. A two-way ANOVA was used to examine the influence of genotype and activation state on RLC phosphorylation content. A Holm-Sidak's post hoc test was used to test for differences of all main effects. Differences were considered significant if $P < 0.05$. Data are presented as means \pm SEM.

Results

Concentric forces of WT and skMLCK $^{-/-}$ muscles

Representative records depicting unpotentiated and potentiated contractions of WT and skMLCK $^{-/-}$ muscles at two different speeds are shown in Fig. 2. Although evident in both genotypes, this example demonstrates the much greater potentiation of concentric force (and thus work and power) of WT muscles at fast speeds compared to skMLCK $^{-/-}$ muscles. In

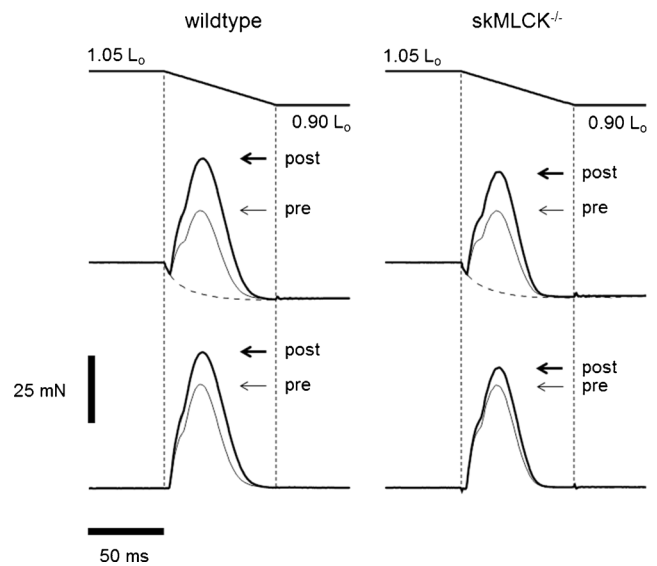


Fig. 2 Concentric forces of WT and skMLCK $^{-/-}$ muscles before and after a PS. Representative force records showing influence of genotype on concentric force potentiation at 0.50 V_{max} of EDL muscles in vitro (25 $^{\circ}$ C). Records from WT muscles shown on the left side and records from skMLCK $^{-/-}$ muscles shown on the right side. Top panel shows the length traces with scale, middle panel shows the pre- and post-PS (unpotentiated and potentiated, respectively) total and active force records superimposed along with passive (dashed line) response, and bottom panel shows the active force records (total-passive) for pre- and post-PS conditions. These records illustrate the effect of the two closely spaced stimulus pulses (i.e., 10 ms), a protocol that produces maximal force development in a short time window compared to single pulses (i.e., twitches) or lower-frequency stimuli [26]. To facilitate comparisons between genotypes, the unpotentiated force records of the skMLCK $^{-/-}$ muscle were scaled to those of the wild-type muscle; the potentiated force records were then adjusted accordingly. In these examples, mean active concentric force was increased by \sim 30 and 15 % in the WT and the skMLCK $^{-/-}$ muscle, respectively. The vertical line depicts the start of ramp shortening. Time and force scales are shown at the bottom. See “Methods” section for more details. For clarity, only one length record and only the unpotentiated passive trace are shown

addition, these records reveal the complete absence of potentiation at slow speeds in skMLCK $^{-/-}$ muscles. The specific tensions measured before and after the PS at each speed for all experiments are compiled in Table 1 for both WT and skMLCK $^{-/-}$ muscles. No statistically significant differences in unpotentiated (i.e., pre-PS) specific tension were detected between genotypes at any speed. In addition, the PS altered the specific tension of muscles at every speed, with the direction and magnitude of change depending on both genotype and shortening speed. The relative increase in these forces at each speed for both genotypes is shown in Fig. 3. These data clearly show the genotype and shortening speed-dependent changes in relative concentric force found during our experiments. For example, concentric force was increased approximately twofold more in WT than in skMLCK $^{-/-}$ muscles at 0.30–0.70 V_{max} . On the other hand, at 0.05–0.20 V_{max} , concentric force was increased in WT muscles but was either

Table 1 Mean stress of EDL muscle from WT and skMLCK^{-/-} mice before and after stimulation

| Genotype | Shortening speed | | | | | | | | |
|-----------------------|------------------|--------------|--------------|--------------|--------------|--------------|--------------|--------------|--------------|
| | Condition | 0.05 | 0.10 | 0.20 | 0.30 | 0.40 | 0.50 | 0.60 | 0.70 |
| WT | Pre-PS | 23.5 ± 1.72 | 20.3 ± 1.81 | 17.5 ± 1.25 | 14.5 ± 1.14 | 12.8 ± 1.08 | 10.4 ± 0.74 | 9.3 ± 0.65 | 7.5 ± 0.68 |
| | Post-PS | 25.3 ± 2.11* | 22.6 ± 2.13* | 20.8 ± 1.70* | 19.1 ± 1.39* | 17.2 ± 1.29* | 14.6 ± 1.08* | 12.6 ± 0.91* | 10.3 ± 0.96* |
| skMLCK ^{-/-} | Pre-PS | 24.2 ± 1.93 | 22.2 ± 1.93 | 18.8 ± 1.71 | 15.2 ± 1.38 | 13.4 ± 1.15 | 11.3 ± 0.85 | 10.3 ± 0.98 | 8.1 ± 0.71 |
| | Post-PS | 21.6 ± 1.38* | 20.7 ± 1.75* | 19.2 ± 1.40 | 17.5 ± 1.47* | 16.1 ± 1.25* | 13.5 ± 1.04* | 12.1 ± 1.02* | 10.0 ± 0.89* |

Values presented as mean ± SEM ($n = 10$). Mean specific tension expressed as g/mm^2 . Shortening speed expressed as V/V_{max} . Relative change is calculated as post-PS value divided by pre-PS value at each speed for each genotype. Intraspeed differences in force were not analyzed for either genotype. No differences in unpotentiated stress were detected between genotypes at any speed

WT wild-type EDL, skMLCK^{-/-} skMLCK devoid EDL

*Within genotype post-PS value different from pre-value ($P < 0.05$)

decreased or unchanged in skMLCK^{-/-} muscles. Thus, distinct differences in concentric force potentiation were observed between genotypes at both fast and slow speeds of shortening.

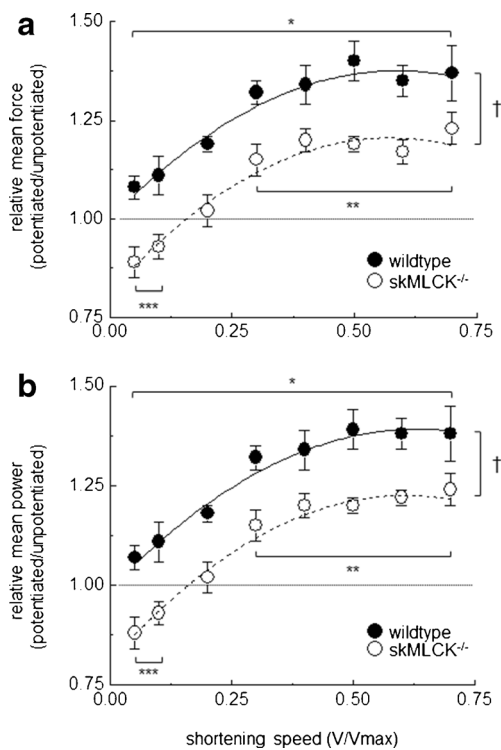


Fig. 3 Force and power of WT and skMLCK^{-/-} muscles before and after a PS. **a** Relative (post-PS/pre-PS) concentric force of WT and skMLCK^{-/-} muscles at each speed tested. Curve fit to WT and skMLCK^{-/-} data set is a second-order polynomial with $r^2 = 0.93$ and 0.94 , respectively. **b** Relative (post-PS/pre-PS) power for WT and skMLCK^{-/-} muscles at each speed tested. Curve fit to WT and skMLCK^{-/-} data set is a second-order polynomial with $r^2 = 0.94$ and 0.98 , respectively. *WT value greater than 1.00 at all speeds ($P < 0.05$). **skMLCK^{-/-} value greater than 1.00 at speeds indicated ($P < 0.05$). ***skMLCK^{-/-} value less than 1.00 at speeds indicated ($P < 0.05$). †WT value different from skMLCK^{-/-} value at all speeds ($P < 0.05$). All values derived from data presented in Tables 1 and 2, respectively

Mean power output of WT and skMLCK^{-/-} muscles The absolute unpotentiated and potentiated values for mean power output of WT and skMLCK^{-/-} muscles are shown in Table 2. Similar values for power were reported by Xenii et al. [41] using the same experimental model and temperature. Similar to our force data, no statistically significant differences in unpotentiated power were detected between genotypes at any speed. The PS did, however, alter power of muscles in a genotype-dependent manner. The relative (post-PS/pre-PS) increase in power output at each speed for each genotype is shown in Fig. 3b. Comparison of the relative force and power data plotted in Fig. 3a, b, respectively, reveals the extent to which power reflected force in our experiments. Moreover, the greatest increases in power caused by the PS were observed at a range of speeds expected to produce the greatest power (i.e., 0.30 – $0.70 V_{\text{max}}$) in both genotypes. At these speeds, power was potentiated in both genotypes but was clearly potentiated a great deal more in WT muscles than in skMLCK^{-/-} muscles. By contrast, at slower speeds (i.e., 0.05 – $0.20 V_{\text{max}}$), power was potentiated only in WT muscles. In terms of peak power ($\text{W} \cdot \text{kg}^{-1}$), output values for both genotypes tended to be approximately twofold greater than mean power at all speeds (data not shown). The genotype-dependent difference we reported for mean power was retained when relative peak power was calculated, however (i.e., WT and skMLCK^{-/-} muscles increased by 21–34 and 7–16 %, respectively). The only difference in this respect was that skMLCK^{-/-} muscles displayed moderate increases, and no decreases, in relative peak power at low speeds of shortening.

The force-velocity responses of WT and skMLCK^{-/-} muscles obtained from muscles before and after the PS are shown in Fig. 4a, b, respectively. Comparison of these plots reveals the extent to which unpotentiated force-velocity characteristics of both genotypes were similar. In contrast, although potentiation greatly reduced the concavity of the force-velocity characteristics of both genotypes, these plots reveal unequivocal genotype-dependent differences. For example, in WT muscles, the difference between unpotentiated and potentiated

Table 2 Mean power output of EDL muscle from WT and skMLCK^{-/-} mice before and after stimulation

| Genotype | Shortening speed | | | | | | | | |
|-----------------------|------------------|------------|------------|-------------|--------------|--------------|--------------|--------------|--------------|
| | Condition | 0.05 | 0.10 | 0.20 | 0.30 | 0.40 | 0.50 | 0.60 | 0.70 |
| WT | Pre-PS | 4.3 ± 0.32 | 7.6 ± 0.68 | 13.1 ± 0.94 | 16.4 ± 1.31 | 19.0 ± 1.63 | 19.7 ± 1.40 | 19.5 ± 1.55 | 19.3 ± 1.74 |
| | Post-PS | 4.6 ± 0.38 | 8.4 ± 0.77 | 15.4 ± 1.24 | 21.6 ± 1.53* | 25.5 ± 1.90* | 27.4 ± 2.00* | 26.9 ± 2.15* | 26.6 ± 2.39* |
| skMLCK ^{-/-} | Pre-PS | 4.4 ± 0.37 | 8.2 ± 0.70 | 13.8 ± 1.20 | 16.9 ± 1.45 | 19.6 ± 1.60 | 21.0 ± 1.57 | 20.7 ± 1.65 | 20.5 ± 1.76 |
| | Post-PS | 3.9 ± 0.28 | 7.6 ± 0.68 | 14.1 ± 1.02 | 19.4 ± 1.61* | 23.6 ± 1.81* | 25.1 ± 1.89* | 25.3 ± 2.07* | 25.5 ± 2.26* |

Values presented as mean ± SEM ($n = 10$). Power calculated as described in “Methods” section and expressed as $W \cdot kg^{-1}$. Shortening speed expressed as V/V_{max} . Relative change is calculated as post-PS value divided by pre-PS value at each speed for each genotype. Intraspeed differences in force were not analyzed for either genotype. No differences in unpotentiated stress were detected between genotypes at any speed

WT wild-type EDL, skMLCK^{-/-} skMLCK devoid EDL

*Within genotype post-PS value different from pre-value ($P < 0.05$)

curves, although present at all speeds, was greatest at intermediate speeds of shortening. In contrast, the difference between the curves was minimal at intermediate speeds of shortening in skMLCK^{-/-} muscles. When combined with the absence or minimal level of potentiation at low and fast speeds of

shortening, respectively, it is clear that genotype-dependent differences in force-velocity characteristics were present in potentiated, but not unpotentiated, muscles.

Force kinetics of WT and skMLCK^{-/-} muscles Absolute values for the rate of concentric force development ($+dF/dt$) are shown in Table 3. Consistent with our force data, no genotype-dependent differences in unpotentiated $+dF/dt$ were detected. Relative changes to $+dF/dt$ are shown in Fig. 5a and show that although increased in both genotypes, these increases were greater for WT than for skMLCK^{-/-} muscles at all speeds. Interestingly, the magnitude of increase to $+dF/dt$ was relatively constant across all speeds in both genotypes (22–28 and 9–16 % in WT and skMLCK^{-/-} muscles, respectively). Absolute values for concentric force relaxation rate ($-dF/dt$) are shown in Table 4 with relative changes shown in Fig. 5b. Similar to our data for $+dF/dt$, no genotype-dependent differences in unpotentiated $-dF/dt$ were observed at any speed. In addition, no consistent genotype-dependent differences in relative $-dF/dt$ were found as this parameter was increased similarly in WT and skMLCK^{-/-} muscles at most speeds. The only exception to this trend was during shortening at $0.05 V_{max}$, where skMLCK^{-/-} muscles displayed a greater relative $-dF/dt$ than WT muscles. Finally, the magnitude of increase to relative $-dF/dt$ caused by the PS was highly speed dependent in both genotypes, being increased more at speeds $\leq 0.30 V_{max}$ than at speeds $\geq 0.40 V_{max}$.

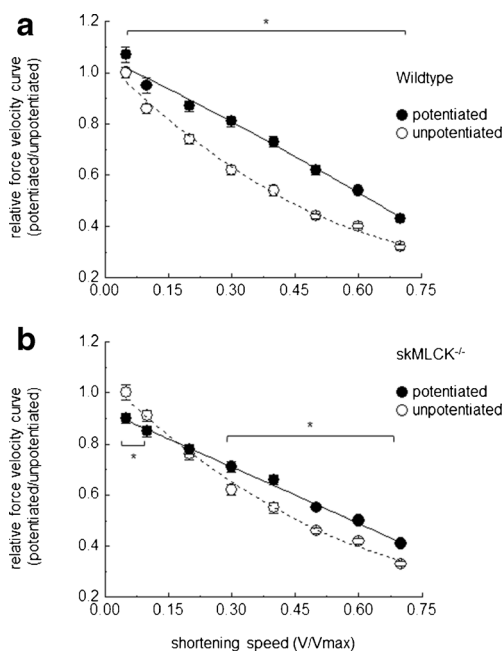


Fig. 4 Power-velocity curves of WT and skMLCK^{-/-} muscles before and after a PS. **a** Relative (post-PS/pre-PS) power-velocity curve for wild-type muscles. Unpotentiated curve was generated by dividing unpotentiated value obtained at each speed by unpotentiated value at $0.05 V_{max}$. Potentiated curve was generated by dividing each potentiated value by unpotentiated value at $0.05 V_{max}$. Curve fits are second-order polynomials with $r^2 \geq 0.99$. **b** Relative (post-PS/pre-PS) power-velocity curve for skMLCK^{-/-} muscles. Unpotentiated curve was generated by dividing unpotentiated value obtained at each speed by unpotentiated value at $0.05 V_{max}$. Potentiated curve was generated by dividing each potentiated value by unpotentiated value at $0.05 V_{max}$. Curve fits are second-order polynomials with $r^2 \geq 0.99$. *Significantly different from 1.00 at speeds indicated ($P < 0.05$). All values derived from data presented in Tables 3 and 4

Myosin RLC phosphorylation A representative blot showing WT and skMLCK^{-/-} data and a graph summarizing all RLC phosphorylation data are shown in Fig. 6. Consistent with previous studies [14, 17, 42], the PS produced large elevations in the RLC phosphorylation of WT but not in skMLCK^{-/-} muscles.

Table 3 Rate of concentric force development of EDL muscle from WT and skMLCK^{-/-} mice before and after stimulation

| Genotype | Shortening speed | | | | | | | | |
|-----------------------|------------------|-------------|-------------|-------------|-------------|-------------|-------------|-------------|-------------|
| | Condition | 0.05 | 0.10 | 0.20 | 0.30 | 0.40 | 0.50 | 0.60 | 0.70 |
| WT | Pre-PS | 2319 ± 254 | 2240 ± 280 | 2047 ± 226 | 1868 ± 232 | 1709 ± 220 | 1536 ± 184 | 1466 ± 179 | 1301 ± 149 |
| | Post-PS | 2875 ± 305* | 2713 ± 302* | 2521 ± 265* | 2313 ± 270* | 2120 ± 262* | 1946 ± 224* | 1790 ± 212* | 1617 ± 204* |
| skMLCK ^{-/-} | Pre-PS | 2250 ± 177 | 2218 ± 181 | 2138 ± 175 | 1934 ± 153 | 1792 ± 133 | 1596 ± 116± | 1515 ± 122 | 1337 ± 112 |
| | Post-PS | 2579 ± 196* | 2497 ± 205* | 2311 ± 167* | 2169 ± 177* | 2034 ± 151* | 1850 ± 131* | 1731 ± 121* | 1515 ± 122* |

Values presented as mean ± SEM ($n = 10$). Rate of concentric force development ($+dF/dt$) calculated as described in “Methods” section and expressed in mN s^{-1} . Shortening speed expressed as V/V_{max} . Relative change is calculated as post-PS value divided by pre-PS value at each speed for each genotype. Intraspeed differences in force not analyzed for either genotype. No differences in unpotentiated stress were detected between genotypes at any speed
WT wild-type EDL, skMLCK^{-/-} skMLCK devoid EDL

*Within genotype post-PS value different from pre-value ($P < 0.05$)

Discussion

Our main finding was that the peak power output of skMLCK^{-/-} muscles was reduced compared to WT mouse EDL muscles, indicating that skMLCK-catalyzed phosphorylation of the RLC is required for attaining maximal concentric

power. For example, of our four main conditions, the potentiated state of wild-type muscles displayed the greatest absolute power. Moreover, although power at all shortening speeds was increased, the biggest relative increase between WT and skMLCK^{-/-} muscles was observed at intermediate shortening speeds producing the most power (in both genotypes). Thus, although skMLCK^{-/-} muscles did potentiate at most speeds, our data indicate that skMLCK-catalyzed phosphorylation of the RLC is required for both submaximal and maximal power of mouse EDL muscle in vitro (25 °C).

The present study supports previous work associating RLC phosphorylation with increased concentric function of mouse fast skeletal muscle. For example, Xeni et al. [41] used mouse EDL to demonstrate correlations between stimulation-induced elevations in RLC phosphorylation and the potentiation of concentric twitch force, work, and power at a fixed shortening speed (i.e., 0.25 V_{max}). The present results extend these observations by showing that, because skMLCK muscles displayed significant deficits in peak power, the skMLCK-catalyzed phosphorylation of the RLC is required for peak power during shortening at fast and slow speeds. The potentiation of power we observed in both genotypes can be attributed to the increased mean concentric force we observed at every speed in WT and at most speeds in skMLCK^{-/-} muscles. Because the shortening ramps we used mimicked the shortening trajectories determined from the muscles from freely moving mice [5, 21, 24], this potentiation is likely to be functional for in vivo locomotion.

An important aspect of the present study is that it confirms previous studies linking the absence of RLC phosphorylation with reduced potentiation in muscles from skMLCK^{-/-} mice. The mechanism responsible for the residual potentiation observed in skMLCK^{-/-} muscles is unknown but may be related to an enhanced Ca^{2+} -activation of the contractile apparatus. For example, elevations in resting myoplasmic Ca^{2+} levels following stimulation have been observed in frog skeletal muscle fibers at cold temperatures [11, 12]. More recently,

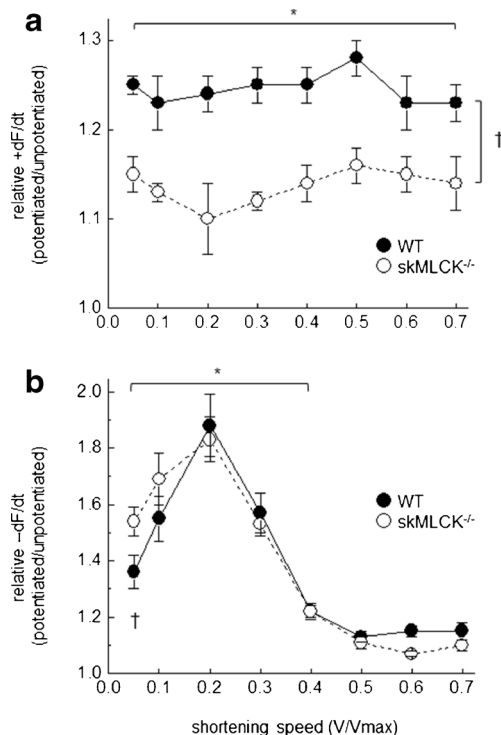


Fig. 5 Concentric force kinetics of WT and skMLCK^{-/-} muscles before and after a PS. **a** Relative (post-PS/pre-PS) rate of concentric force development ($+dF/dt$) for WT and skMLCK^{-/-} muscles. Respective curves derived by dividing post-PS responses by pre-PS responses at each speed (within genotype). **b** Relative (post-PS/pre-PS) rate of concentric force relaxation ($-dF/dt$) for WT and skMLCK^{-/-} muscles. *WT or skMLCK^{-/-} potentiated value different from 1.00 (unpotentiated) value at speeds indicated ($P < 0.05$). †WT value different from skMLCK^{-/-} value at that speed ($P < 0.05$). All values derived from data presented in Tables 3 and 4, respectively

Table 4 Rate of concentric force relaxation of EDL muscle from WT and skMLCK^{-/-} mice before and after stimulation

| Genotype | Shortening speed | | | | | | | | |
|-----------------------|------------------|-------------|-------------|-------------|-------------|-------------|-----------|-----------|-----------|
| | Condition | 0.05 | 0.10 | 0.20 | 0.30 | 0.40 | 0.50 | 0.60 | 0.70 |
| WT | Pre-PS | 1290 ± 118 | 1108 ± 106 | 868 ± 82 | 845 ± 82 | 829 ± 84 | 813 ± 73 | 662 ± 67 | 659 ± 66 |
| | Post-PS | 1761 ± 191* | 1713 ± 184* | 1616 ± 173* | 1301 ± 116* | 1002 ± 92* | 916 ± 83* | 760 ± 76* | 751 ± 67* |
| skMLCK ^{-/-} | Pre-PS | 1115 ± 157 | 989 ± 124 | 845 ± 86 | 818 ± 78 | 826 ± 77 | 780 ± 67 | 747 ± 69 | 648 ± 69 |
| | Post-PS | 1708 ± 246* | 1690 ± 246* | 1580 ± 213* | 1286 ± 164* | 1019 ± 113* | 870 ± 84* | 804 ± 77* | 712 ± 77* |

Values presented as mean ± SEM ($n = 10$). Rate of concentric force relaxation ($+dF/dt$) calculated as described in “Methods” section and expressed in $mN s^{-1}$. Shortening speed expressed as V/V_{max} . Relative change is calculated as post-PS value divided by pre-PS value at each speed for each genotype. Intraspeed differences in force not analyzed for either genotype. No differences in unpotentiated stress were detected between genotypes at any speed
 WT wild-type EDL, skMLCK^{-/-} skMLCK devoid EDL

*Within genotype post-PS value different from pre-value ($P < 0.05$)

Smith et al. [34] showed that the potentiation of isometric twitch force following high-frequency stimulation was associated with elevations in resting myoplasmic Ca^{2+} levels ($[Ca^{2+}]_i$) in the mouse lumbrical muscle (at 37 °C). Mechanistically, elevations in resting $[Ca^{2+}]_i$ may “pre-load” or saturate intracellular Ca^{2+} buffers, an effect that may bias Ca^{2+} binding to TnC. On the other hand, Abbate et al. [3] did not find any evidence that the potentiation caused by a high-frequency volley alters resting $[Ca^{2+}]_i$ of intact mouse flexor

brevis fibers. Nevertheless, it seems possible to hypothesize that the residual potentiation displayed by skMLCK^{-/-} muscles or by denervated or disused fast rat skeletal muscle is due to this or a related mechanism [27, 32].

Force kinetics Inspection of the data in Tables 3 and 4 and Fig. 5 make clear that the PS dramatically altered force kinetics in both genotypes. Although we used tetanic (100 Hz) stimulation, each contraction was brief and consisted of only two pulses; our force profiles are very comparable to twitch contractions. In this regard, potentiated isometric twitches have been shown to display enhanced rates of force development that are strongly correlated with RLC phosphorylation [38, 39]. Although the relative increase in $+dF/dt$ caused by the PS was uniform across all shortening speeds tested for each genotype (Fig. 5), this parameter was higher in WT muscles than in skMLCK^{-/-} at every speed tested. Thus, although there is a RLC phosphorylation-independent component, the nature of which is unknown; RLC phosphorylation is required for maximal $+dF/dt$. In addition, consistent with previous studies, the muscles of both genotypes displayed increases in relative $-dF/dt$ at all speeds following the PS [15]. This increase in relative $-dF/dt$ was similar in both genotypes at shortening speeds equal to or above 0.10 V_{max} , suggesting that this effect was largely independent of RLC phosphorylation. Changes of this order to this parameter may have significant ramifications for force development during unfused or partially fused contractions. Indeed, the large increases in relative $-dF/dt$ observed in both genotypes at slow speeds of shortening may have reduced concentric force summation of skMLCK^{-/-} muscles; in contrast, because the change to relative $-dF/dt$ was not as great and the change in relative $+dF/dt$ was greater, alterations to force kinetics did not mitigate force potentiation to as great a degree in WT muscles.

The interactions between force kinetics and potentiation we observed in WT and skMLCK^{-/-} muscles may suggest a role for RLC phosphorylation in modulating force summation

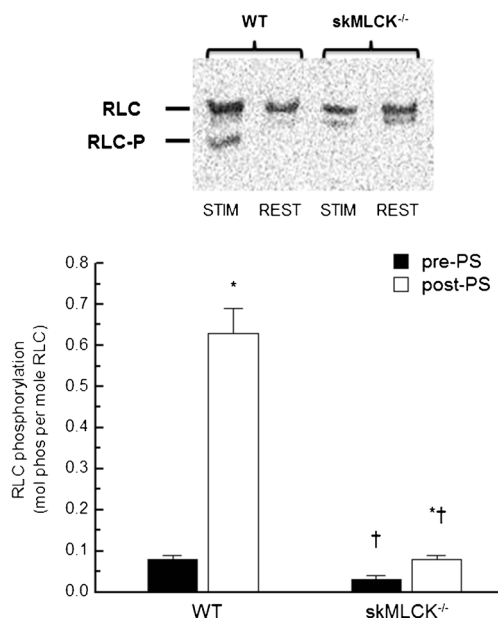


Fig. 6 RLC phosphorylation in WT and skMLCK^{-/-} muscles before and after a PS. **a** Representative urea/glycerol PAGE blot of phosphorylated and non-phosphorylated myosin RLC from individual WT and skMLCK^{-/-} mouse EDL muscle. The blot shows how the PS produced an easily detected phosphorylated band in WT but not skMLCK^{-/-} muscles. The middle band is an unidentified protein (see [42] and [33] for discussion). **b** Summary data for RLC phosphorylation for WT and skMLCK^{-/-} muscles at rest (pre-PS, open bars) and after (post-PS, black bars) stimulation. Values are presented as mean and ±SEM ($n = 4$). *Significantly different from the rest (pre-PS) ($P < 0.05$). †skMLCK^{-/-} value different from WT value within that condition ($p < 0.05$)

during unfused contractions. Because skMLCK^{-/-} muscles displayed greater increases in relative $-dF/dt$ than did WT muscles at 0.05 V_{\max} , we are tempted to suggest that RLC phosphorylation slowed relaxation rate at these speeds (i.e., the change in relative $-dF/dt$ was not as great). Indeed, RLC phosphorylation has been associated with a slowed relaxation rate from high-force contractions in intact mouse and cat muscle (e.g., [10, 14]) as well as in permeabilized rabbit skeletal fibers [30]. Although the mechanism for any such effect is unclear, it may mitigate reductions in force due to contraction-mediated increases in relaxation rate of murine fast twitch skeletal muscle.

Peak power and shortening speed The shortening speed at which mechanical power is maximized is a key feature of skeletal muscle function (e.g., [6]). Work on rat skeletal muscle in situ has shown that the velocity at which power peaks is shifted to a higher fraction of V_{\max} in the potentiated state [2]. We did not observe this effect in our experiments, however, as peak power occurred at the same shortening speed in both the unpotentiated and potentiated states for both genotypes. This may have been related to the fact that our power-velocity curves displayed a very broad peak of values over 0.35–0.55 of V_{\max} compared to other studies (e.g., [8]). Because stimulation timing and parameters were held constant throughout, active force development encompassed a lower percent of overall shortening amplitude at low compared to fast speeds. Thus, the peak of concentric force development occurred at slightly shorter muscle lengths at slow than at fast speeds. Also, although we have been unable to detect a length dependence for concentric force potentiation when examined within the same contraction [16, 41], the possibility remains that a length dependence for concentric force potentiation exists as it does for isometric potentiation [32]. If so, this effect may have obviated our ability to detect shifts in the power-velocity relationship with potentiation. Finally, even though we did not attempt to control sarcomere length, our experimental conditions likely mimic in vivo conditions to a greater degree than experiments in which sarcomere length is controlled.

Limitations to genetic model Previous work has shown no apparent differences between EDL muscles of WT and skMLCK^{-/-} muscles in terms of contractile performance or fiber type [14, 33, 34, 42]. Because it was not higher than that observed in unstimulated WT muscles, the RLC phosphorylation observed in stimulated skMLCK^{-/-} muscles was assumed to be non-modulatory in nature. As a result, we have interpreted our results under the assumption that the presence of skMLCK-catalyzed phosphorylation of the RLC, and attendant increases in the Ca^{2+} sensitivity of force development, was the main/only phenotype difference between WT and skMLCK^{-/-} muscles. The corollary to this assumption is that the mechanism for the residual potentiation displayed by

skMLCK^{-/-} muscles was also present in WT muscles. An important caveat to the above assumptions is that we cannot rule out adaptations in the transcriptome of skMLCK^{-/-} muscles that renders these assumptions invalid. Indeed, little can be known regarding how “rescuing” RLC phosphorylation in skMLCK^{-/-} muscles would modulate contraction beyond that which is already apparent. More work comparing the identity of the fast phenotype gene program in wild-type and skMLCK ablated mice is needed before the deficits associated with the absence of RLC phosphorylation in skMLCK^{-/-} muscles can be established with absolute certainty.

In summary, we found that ablation of the skMLCK gene and absence of RLC phosphorylation reduce the maximal possible power output of mouse fast muscle. Thus, although skMLCK^{-/-} muscles display an RLC phosphorylation-independent form of potentiation, their peak contractile function is impaired compared to wild-type muscles. Because skMLCK-catalyzed phosphorylation of the RLC is required for maximal concentric force, work, and power, our results suggest that this molecular mechanism may occupy an important biological role for muscle function in vivo.

Acknowledgments This study was supported by funds provided by the Natural Sciences and Engineering Research Council of Canada to R.V. (no. 2014-05122).

Compliance with ethical standards

Conflict of interest The authors declare that they have no conflict of interest.

References

1. Abbate F, Sargeant AJ, Verdijk PW, de Haan A (2000) Effects of high-frequency initial pulses and posttetanic potentiation on power output of skeletal muscle. *J Appl Physiol* 88:35–40
2. Abbate F, Van Der Velden J, Stienen GJ, De Haan A (2001) Posttetanic potentiation increases energy cost to a higher extent than work in rat fast skeletal muscle. *J Musc Res Cell Motil* 22: 703–710
3. Abbate F, Bruton JD, De Haan A, Westerblad H (2002) Prolonged force increase following a high-frequency burst is not due to a sustained elevation of $[Ca^{2+}]_i$. *Am J Physiol Cell Physiol* 283(1): C42–C47
4. Alamo L, Qi D, Wriggers W, Pinto A, Zhu J, Bilbao A, Gillilan RE, Hu S, Padron R (2016) Conserved intramolecular interactions maintain myosin interacting-heads motifs explaining tarantula muscle super-relaxed state structural basis. *J Mol Biol* 428:1142–1164
5. Askew GN, Marsh RL (1997) The effects of length trajectory on the mechanical power output of mouse skeletal muscles. *J Exp Biol* 200(24):3119–3131
6. Askew GN, Marsh RL (1998) Optimal shortening velocity (V/V_{\max}) of skeletal muscle during cyclical contractions: length-force effects and velocity-dependent activation and deactivation. *J Exp Biol* 201(Pt 10):1527–1540

7. Barclay CJ (2005) Modelling diffusive O₂ supply to isolated preparations of mammalian skeletal and cardiac muscle. *J Musc Res Cell Motil* 26:225–235
8. Brooks SV, Faulkner JA, McCubrey DA (1990) Power outputs of slow and fast skeletal muscles of mice. *J Appl Physiol* 68(3):1282–1285
9. Brown IE, Loeb GE (1998) Post-activation potentiation: a clue for simplifying models of muscle dynamics. *Am Zool* 38(4):743–754
10. Brown IE, Loeb GE (1999) Measured and modeled properties of mammalian skeletal muscle. I. The effects of post-activation potentiation on the time course and velocity dependencies of force production. *J Musc Res Cell Motil* 20:443–456
11. Cannell MB (1986) Effect of tetanus duration on the free calcium during the relaxation of frog skeletal muscle fibres. *J Physiol* 1986(376):203–218
12. Caputo C, Edman KA, Lou F, Sun YB (1994) Variation in myoplasmic Ca²⁺ concentration during contraction and relaxation studied by the indicator fluo-3 in frog muscle fibres. *J Physiol* 478(Pt 1):137–148
13. Caterini D, Gittings W, Huang J, Vandenboom R (2011) The effect of work cycle frequency on the potentiation of dynamic function in fast mouse muscle. *J Exp Biol* 214:3915–3923
14. Gittings W, Huang J, Smith I, Quadrilatero J, Vandenboom R (2011) The influence of myosin light chain kinase (MLCK) gene ablation on the contractile performance of skeletal muscles during fatigue. *J Musc Res Cell Motil* 31:337–348
15. Gittings W, Huang J, Vandenboom R (2012) Tetanic force potentiation of mouse fast muscle is shortening speed dependent. *J Musc Res Cell Motil* 33(5):359–368
16. Gittings W, Aggarwal H, Stull JT, Vandenboom R (2015) The force dependence of isometric and concentric potentiation in mouse muscles with and without myosin light chain kinase. *Can J Physiol Pharmacol* 93(1):23–32
17. Gittings W, Stull JT, Vandenboom R (2016) Interactions between the catch like property and posttetanic potentiation of mouse skeletal muscle. *Muscle Nerve* 54(2):308–316
18. Grange RW, Cory CR, Vandenboom R, Houston ME (1995) Myosin phosphorylation augments the force-displacement and force-velocity relationships of mouse fast muscle. *Am J Phys* 269:C713–C724
19. Grange RW, Vandenboom R, Xenii J, Houston ME (1998) Potentiation of in vitro concentric work in mouse fast muscle. *J Appl Physiol* 84:236–243
20. Grange RW, Gainer TG, Marschner KM, Talmadge RJ, Stull JT (2002) Fast-twitch skeletal muscles of dystrophic mouse pups are resistant to injury from acute mechanical stress. *Am J Physiol-(Cell Physiol)* 283(4):C1090–C1101
21. James RS, Altringham JD, Goldspink DF (1995) The mechanical properties of fast and slow skeletal muscles of the mouse in relation to their locomotory function. *J Exp Biol* 198(2):491–502
22. Josephson RK (1999) Dissecting muscle power output. *J Exp Biol* 202:3369–3375
23. Lannergren J, Bruton JD, Westerblad H (2000) Vacuole formation in fatigued skeletal muscle fibres from frog and mouse: effects of extracellular lactate. *J Physiol* 526(3):597–611
24. Leblond H, L'Esperance M, Orsal D, Rossignol S (2003) Treadmill locomotion in the intact and spinal mouse. *J Neurosci* 23:11411–11419
25. MacIntosh BR, Bryan SN (2002) Potentiation of shortening and velocity of shortening during repeated isotonic tetanic contractions in mammalian skeletal muscle. *Pflugers Arch* 443:804–812
26. MacIntosh BR, Willis JC (2000) Force-frequency relationship and potentiation in mammalian skeletal muscle. *J Appl Physiol* 88(6):2088–2096
27. MacIntosh BR, Smith MJ, Rassier DE (2008a) Staircase but not posttetanic potentiation in rat muscle after spinal cord hemisection. *Muscle Nerve* 38(5):1455–1465
28. MacIntosh BR, Taub EC, Dormer GN, Tomaras EK (2008b) Potentiation of isometric and isotonic contractions during high-frequency stimulation. *Pflugers Arch* 456:449–458
29. Mendez J, Keys A (1960) Density and composition of mammalian muscle. *Metabolism-Clinical and Experimental* 9(2):184–188
30. Patel JR, Diffie GM, Huang XP, Moss RL (1998) Phosphorylation of myosin regulatory light chain eliminates force-dependent changes in relaxation rates in skeletal muscle. *Biophys J* 74:360–368
31. Persechini A, Stull JT, Cooke R (1985) The effect of myosin phosphorylation on the contractile properties of skinned rabbit skeletal muscle fibers. *J Biol Chem* 260:7951–7954
32. Rassier DE, Tubman LA, MacIntosh BR (1999) Staircase in mammalian muscle without light chain phosphorylation. *Braz J Med Biol Res* 32(1):121–129
33. Ryder JW, Lau KS, Kamm KE, Stull JT (2007) Enhanced skeletal muscle contraction with myosin light chain phosphorylation by a calmodulin-sensing kinase. *J Biol Chem* 282:20447–20454
34. Smith I, Gittings W, Bloemberg D, Huang J, Quadrilatero J, Tupling AR, Vandenboom R (2013) Potentiation in mouse lumbrical muscle without myosin light chain phosphorylation: is resting calcium responsible? *J Gen Physiol* 141(3):297–308
35. Stull JT, Kamm C, Vandenboom R (2011) Myosin light chain kinase and the role of myosin light chain phosphorylation in skeletal muscle. *Arch Biochem Biophys* 510:120–128
36. Tsianos GA, Rustin C, Loeb GE (2012) Mammalian muscle model for predicting force and energetics during physiological behaviors. *Neural Systems and Rehabilitation Engineering, IEEE Transactions* 20(2):117–133
37. Vandenboom R, Grange RW, Houston ME (1993) Threshold for force potentiation associated with skeletal myosin phosphorylation. *Am J Phys* 265(6 Pt 1):C1456–C1462
38. Vandenboom R, Grange RW, Houston ME (1995) Myosin phosphorylation enhances rate of force development in fast-twitch skeletal muscle. *Am J Phys* 268:596–603
39. Vandenboom R, Xenii J, Bestic M, Houston ME (1997) Increased force development rates of fatigued skeletal muscle are graded to myosin light chain phosphate content. *Am J Phys* 272:1980–1984
40. Vandenboom R, Gittings W, Smith IC, Grange RW, Stull JT (2013) Myosin phosphorylation and force potentiation in skeletal muscle: evidence from animal models. *J Musc Res Cell Motil* 34(5–6):317–332
41. Xenii J, Gittings W, Caterini D, Huang J, Houston ME, Grange RW, Vandenboom R (2011) Myosin light chain phosphorylation and potentiation of dynamic function in mouse fast muscle. *Pflugers Archiv* 362:349–358
42. Zhi G, Ryder JW, Huang J, Ding P, Chen Y, Zhao Y, Kamm KE, Stull JT (2005) Myosin light chain kinase and myosin phosphorylation effect frequency-dependent potentiation of skeletal muscle contraction. *Proc Natl Acad Sc USA* 102:17519–17524